Machined Brass and Pressed Steel Bearing Cages: a Comparative Study

Spiridon CRETU
RKB Bearing Industries – Engineering and Research Department

Abstract: *The international standards ISO 281:2007 and ISO 16281:2008 estimate bearings basic dynamic rating loads and basic rating lives on the basis of subsurface contact fatigue of raceways. A life modification factor, a_{ISO}, is further considered in these standards to include surface originated fatigue and correspondingly to evaluate the modified rating lives, but with any implication of cage design and material (brass or steel). Anyway, statistics reveal that only a small percentage of bearing failures is due to subsurface fatigue. Fluctuations in cage speed generate high forces of inertia and skewing motion alters roller-cage contact to the harmful edge contact. These effects give rise to considerable pressure between cage contacting surfaces, that, for rolling bearings equipped with steel cages and operating in conditions of poor lubrication, may lead to adhesive wear and smearing. The hard steel contaminants that may appear, as well as the indentations that may form on raceways and rolling elements, act as locations for surface fatigue, causing a much shorter life than that calculated using ISO 281:2007. In such cases bearings appear as being damaged by surface fatigue but actually the true origin of the failure lies in the adhesive wear of the steel cage. On the contrary, brass cages have a much higher resistance to adhesive bonding and, for this reason, even in harsh conditions, when lubrication is insufficient, they enable bearings to attain the design rating life.*

Key words: *contact fatigue, adhesive wear, machined brass cage, pressed steel cage, impact forces, smearing, bearing cage*

1 INTRODUCTION

As common knowledge, bearing designers use the resistance to depth initiated fatigue as the main criterion to optimize bearing internal macro geometry, represented by the number and size of rolling elements, internal contact geometry and ring thickness. Currently ISO 281:2007 and ISO 16281:2008 estimate the dynamic load ratings based on the same failure criterion and consequently the proposed equations contain no differences regarding cage design and cage material (brass or steel).

With the improvement of bearing steel quality, especially after 1980, the failure of rolling contacts has been observed to initiate from the surface [1]-[3], and the micro geometry of the contacting surfaces has become more and more crucial in rolling bearing technology [4], [5]. Fatigue initiated from the surface is mainly caused by surface distress, that is the damage to the rolling contact metal surface asperities. Particle contamination dents represent surface stress risers and act as locations for incipient surface fatigue [2], [4]-[8]. The modified rating life equation, as formulated by ISO 281:2007, contains the modification factor a_{ISO} that, based on a systems approach to life calculation, quantifies the quality of lubrication and the effects of contaminants.

Since sliding cannot be eliminated in the contacts between the cage and other bearing parts, the cage itself is the first component to be affected when lubrication becomes inadequate. When the rolling bearing is equipped with a pressed steel cage, hard contaminants might appear as a result of the adhesive wear at the cage-rolling element contact.

Although much less effort has been made to analyze cage wear and cage structural fatigue in comparison with that to study rolling contact fatigue, in the last decade scientific literature has been witnessing a significant increase of researches for a better understanding of cage role and dynamics [9]-[18].

2 ROLLING CONTACT FATIGUE: A COMPETITION

2.1 Depth initiated contact fatigue

In rolling bearings the applied load is distributed to rolling elements by concentrated contacts, inducing elevated elastic stresses on the common contacting surfaces as well as inside the loaded materials. The change in the material structure, caused by the repeated stresses developed in the contacts between the rolling elements and the raceways, is described as fatigue. Von Mises equivalent stress as well as orthogonal and Tresca tangential stresses have their maxima under the contacting surface. The full lines of Fig. 1 exemplify the evolution of the Tresca shear stress normalized by the Hertzian pressure, whereas the dashed lines represent the characteristic shear stresses below which no crack initiation and propagation occur. In the areas where these characteristic stresses are overcome, structural changes occur and micro-cracks initiate. Under normal operating conditions, pure sub-surface fatigue does not occur frequently and, in any case, only after a very long running time.

The international standards ISO 281:2007 [6] and ISO 16281:2008 [7] estimate the bearings dynamic load rating *C* based on subsurface rolling contact fatigue. For a certain operating condition a dynamic equivalent load *P* is used to evaluate the basic rating life L_{10}:

$$L_{10} = \left(\frac{C}{P}\right)^{p} \tag{1}$$

2.2 Surface initiated contact fatigue

Fatigue initiated from the surface is caused, among other things, by surface distress, that is the damage to the rolling contact metal surface asperities under a reduced lubrication regime and a certain percentage of sliding motion, causing the formation of asperity micro-cracks, asperity micro-spalls, and micro-spalled areas. In order to eliminate the surface contact fatigue as well as to decrease the friction within the bearing, the micro geometry of the contacting surfaces have to be optimized in correlation with the thickness of the elasto-hydrodynamic lubricant film [1], [3]-[5]. Therefore, if the rolling bearing has been properly designed, manufactured, selected, mounted and lubricated the potential for the occurrence of surface initiated fatigue is virtually nil. However, industry data reveal that the main causes of rolling bearing failures are surface originated and caused above all by inadequate lubrication and contamination [1], [19].

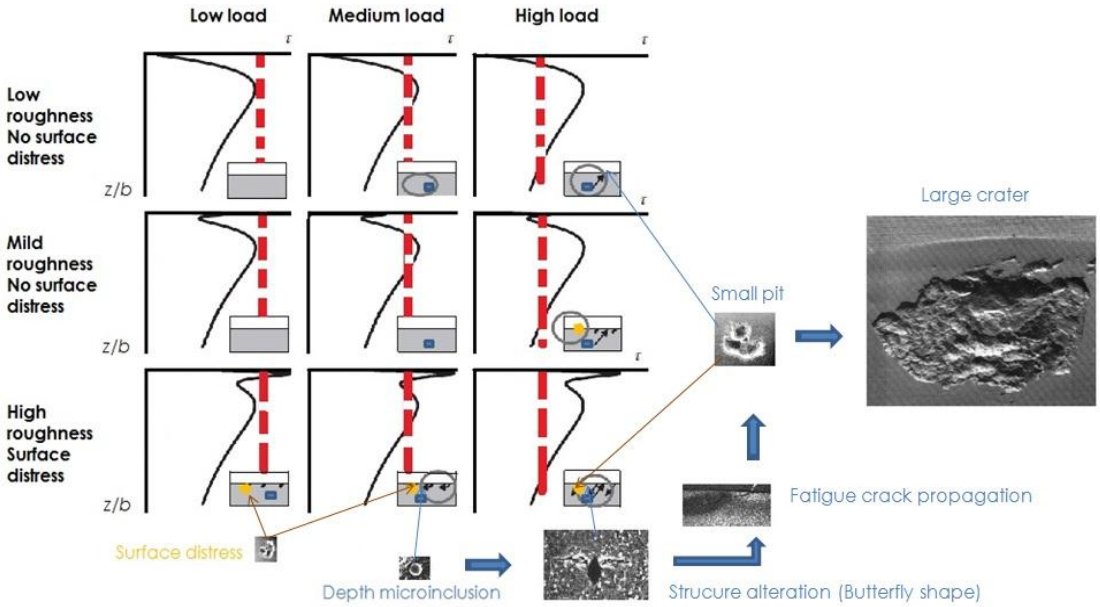

Fig. 1 – Competition between surface and subsurface contact fatigue phenomena

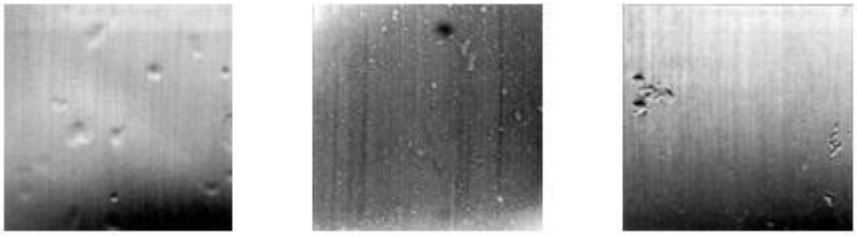

a) b) c)

Fig. 2 – Indentations caused by over-rolled: a) soft particles (e.g. fibers and wood); b) hardened steel particles (e.g. gears and bearings); c) hard mineral particles (e.g. grinding wheels)

2.3 Contaminant particles

When unwanted contaminant particles, present in the lubricant, are over-rolled, indentations form on both raceways and rolling elements. The size and shape of the indentations depend on the nature of the contaminant particles (Fig. 2) [8]. Particle contamination dents represent surface stress risers and act as locations for incipient surface fatigue. This may lead to the rapid failure of the bearing and correspondingly to a shorter service life compared to design life.

The international standard ISO 281:2007, in addition to load, includes surface-related calculation parameters that are known to have an influence on bearing life, such as material, lubrication, environment, contaminant particles, and misalignment. Based on a systems approach to life calculation, a life modification factor, a_{ISO}, is introduced to obtain the modified rating life L_{10m}:

$$L_{10m} = a_{ISO} L_{10} \tag{2}$$

where the life modification factor, a_{ISO}, is derived from the equation:

$$a_{ISO} = f\left(\frac{e_C C_u}{P}, \kappa\right) \tag{3}$$

The factors e_C and κ take into consideration contamination and lubrication conditions respectively, whereas C_U is defined as the load at which the fatigue stress limit is just attained.

The influence of both edge effect and misalignment on basic dynamic load rating as well as the influence of bearing clearance on life are further considered in the international standard ISO 16281:2008.

3 BASIC CAGE DESIGNS

As previously revealed, the international standard ISO 281:2007 considers the subsurface rolling contact fatigue as the main reliability criterion of rolling bearings and consequently provides the appropriate formulae to estimate the basic dynamic load ratings and corresponding basic rating lives. Since for roller bearings the basic rating life is proportional to the number of rollers powered 2.5, the various cage designs try to increase as much as possible the number of rollers to obtain a longer basic rating life.

3.1 Full complement design

The maximum number possible of rollers to be incorporated in a bearing is attained in the full complement bearing design. In this kind of arrangement the direct contact of adjacent rollers causes sliding and increases friction with resulting heat generation and wear, making full complement bearings unsuitable for relatively high speed applications.

3.2 Machined brass cage

As a standard, the RKB Group equips its medium and large size roller bearings with machined brass cage, mainly to keep rollers from making contact and to guide them in the unloaded zone. Cage bridges (Fig. 3 a), which are usually orientated around the roller pitch circle, have the cross section designed to assure both a high bending strength and reduced contact pressure at the impact with a steel rolling element. Compared to steel cages, brass cages machined from centrifugally cast tubing have the advantages:

- Very good balance and absence of dangerous residual stresses.
- Higher limiting speeds.

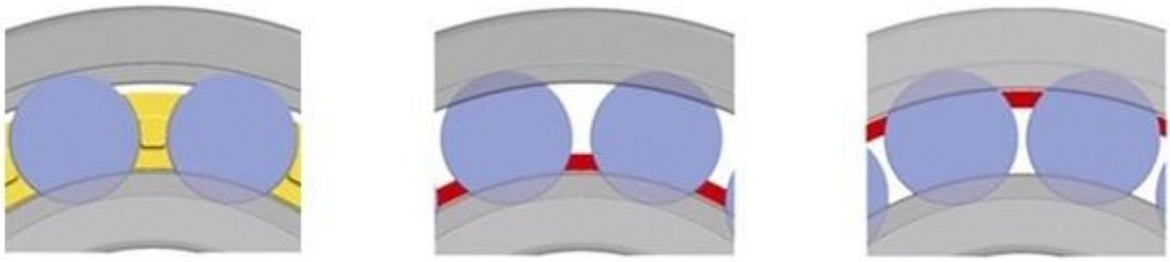

a) b) c)

Fig. 3 – Cylindrical roller bearings with: a) machined brass cage; b–c) window-type pressed steel cage

- Lower vibration and noise characteristics.
- Better lubrication conditions in roller-cage contact area.
- Very good resistance to adhesive wear in roller-cage contact area.
- Increased service life in harsh conditions and boundary lubrication.
- Longer service life under reversing loads.
- Non-susceptibility to chemical stress cracking.

The harmful effect of thermal expansion on cage strength is eliminated in the two-piece machined brass cage, manufactured as a pronged cage with cover.

3.3 Window-type steel cage

In the window-type steel design cage bridges are moved away from the roller pitch circle. Two basic cage designs are the inner ring shoulder guided cage (Fig. 3 b) and the outer ring shoulder guided cage (Fig. 3 c).

Compared to the machined brass design (Fig. 3 a), the window-type cage incorporates more rollers that, for the same basic standardized dimensions, provides a greater dynamic load rating.

The window-type steel cage is lighter and cheaper than the machined brass cage, but with a certain affinity to adhesive wear in roller-cage contact area.

4 BEARING DAMAGES DUE TO CAGE FAILURE

Rarely the cage is found to be the only damaged element in a failed rolling bearing. In fact, usually a damaged cage is accompanied by damages to other rolling bearing elements. The main causes of cage failure lie in vibrations, excessive speed, blockage and different forms of wear.

4.1 Vibrations

When a bearing is exposed to vibrations, the forces of inertia may be so great as to cause fatigue cracks to form in the cage material after a certain time. Sooner or later these cracks may lead to cage fracture. In case of strong shock loads or vibrations, press steel cages are inadequate.

4.2 Excessive speed

If the bearing is run at speeds exceeding that for which its cage is designed, the cage is subjected to heavy forces of inertia that may lead to fractures. Frequently, where very high speeds are involved, it is possible to select bearings with cages of special design.

4.3 Blockage

Fragments of flaked material or other hard particles may become wedged between the cage and a rolling element, preventing the latter from rotating around its own axis and leading to cage failure.

4.4 Wear

Rolling bearings were invented to replace the sliding motion with rolling motion, which means a two orders of magnitude reduction of the corresponding friction coefficient. However, sliding cannot be eliminated at the contacts between the cage and the other components of the bearing. This explains why the cage is the first component to be affected when the lubrication becomes inadequate. The cage is manufactured of softer material than rings and rolling elements and consequently it wears comparatively quickly. As a result the rolling element guidance deteriorates and the resultant forces may lead to cage failure.

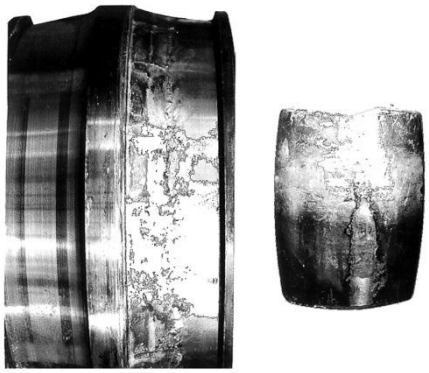

Fig. 4 – Discolored and melted running surfaces due to rolled wear particles from steel cage

When the rolling bearing is equipped with a steel cage, hard contaminants might appear as a result of the adhesive wear at the cage-rolling element contact. This form of adhesive wear, known as smearing, is defined as the transfer of component surface material in visible patches from a location on one surface to a location on the contacting surface, and possibly back onto the original surface. These particles, resulting from the wear process, contaminate the lubricant and become trapped between the rolling elements and raceways. When particles are over-rolled, indentations form on raceways and rolling elements. As previously pointed out, these dents act as locations for surface fatigue causing a much shorter life than that calculated using ISO 281:2007 and based on subsurface fatigue.

When particles from a steel cage attach to the ring raceways and operation continues, there is a high risk of a catastrophic failure. Fig. 4 shows the inner ring of a spherical roller bearing having the running surfaces discolored and melted due to the steel wear particles from the cage [8]. In such cases, the bearings appear as being damaged by surface fatigue but in fact the true origin lies in the wear of steel cage that generates detrimental hard worn particles. Smearing is a welding phenomenon involving adhesive bonding between material portions of the contacting surfaces. This transfer of material takes place because of high-friction shear forces due to sliding over the surface asperities.

Normally, the impact between cage and rolling elements occurs in conditions characterized by significant sliding velocities and boundary lubrication. These normal working conditions may generate adhesive wear or even smearing if accompanied by a high contact pressure, which is determined by roller skewing (that is a kinematics alteration) or greatly increased impact forces due to bad bearing dynamics.

Regarding the cage-roller contact, some of these conditions will be discussed in the following.

5 KINEMATICS OF THE ROLLING ELEMENT-CAGE CONTACT

5.1 Bearing kinematics for moderate speed conditions

In most applications, particularly those operating at relatively slow shaft or outer ring speeds, the internal speeds can be calculated with sufficient accuracy using simple kinematical relationships, that is balls or rollers are assumed to roll on the raceways without sliding [1], [3]. Conditions of pure rolling motions of the ball (Fig. 5) on both outer and inner raceway (points *E* and *I* respectively) provide the equations to obtain the angular speeds ω_c and ω_w for cage and ball respectively:

$$\omega_c = \frac{\omega_e(1+\gamma) + \omega_i(1-\gamma)}{2} \tag{4}$$

$$\omega_w = \frac{D_{pw}}{2D_w}(\omega_e - \omega_i)(1-\gamma^2) \tag{5}$$

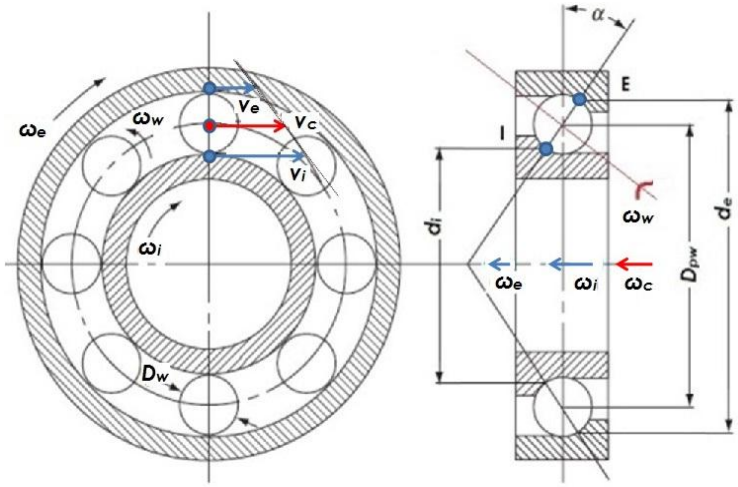

Fig. 5 – Simple kinematics for moderate speed conditions

The rolling element with the angular velocity ω_w around its own axis touches the cage with a sliding velocity:

$$v_{c-w} = \frac{1}{2} D_w \omega_w \tag{6}$$

5.2 Skewing in roller bearings

The skewing and tilting motions occur in the orthogonal planes that contain the roller axis [9]-[14]. In a misaligned bearing, each roller carrying a load is squeezed at one end and forced against the opposing flange with a load Q_{aj}, creating a friction force μQ_{aj} at the roller end (Fig. 6) [9].

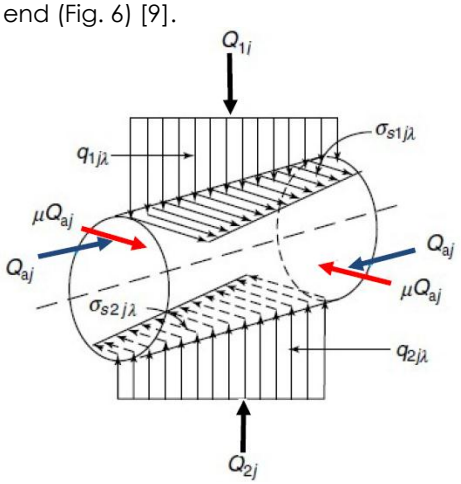

Fig. 6 – Roller skewing in misaligned cylindrical roller bearing

When cylindrical rollers are subjected to axial load Q_a (Fig. 7), due to sliding motions between roller ends and ring flanges, friction forces μQ_a occur (μ is the coefficient of friction).

Because of the friction forces μQ_{aj}, a moment takes place creating, in addition to the predominant rolling motion about the roller axis, a skewing motion and secondary roller tilting. For a bearing with a substantially robust and rigid cage, the skewing angle may be limited by the clearances between the rollers and the cage pockets. For a bearing with guide flanges, the skewing may be limited by the endplay between roller ends and guide flanges [9], [14].

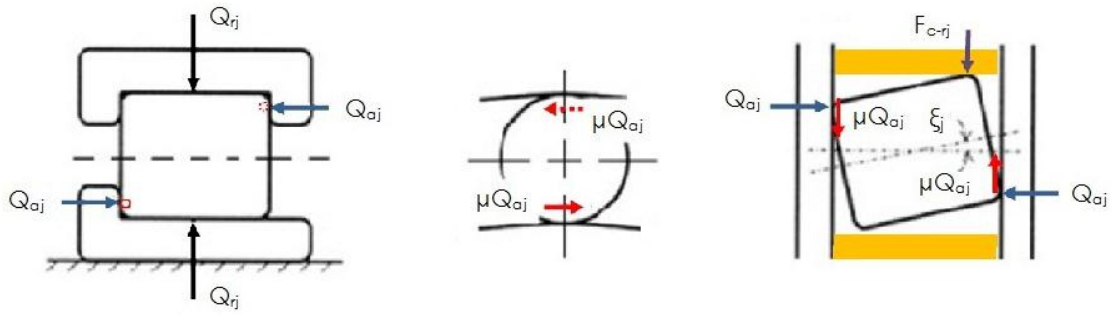

Fig. 7 – Roller skewing in cylindrical roller bearing

In the absence of skewing, rollers get in touch with cage bridges along a line represented by roller generatrix. The presence of skewing motion alters the mentioned line contact to an edge type contact (Fig. 7) that is harmful because of the much higher pressure developed by the interaction force $F_{c\text{-}rj}$:

Skewing motion can also take place in spherical roller bearings (Fig. 8) [10] and tapered roller bearings [11].

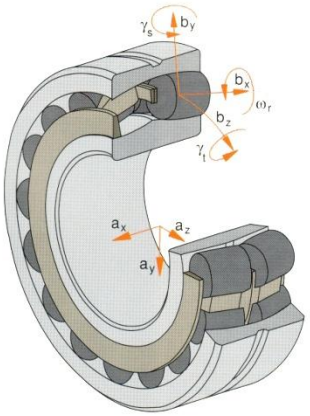

Fig. 8 – Skewing and tilting of roller in spherical roller bearing

Complex studies carried out by Sakaguchi and Harada [15], Houpert [16], [17], and Ghaisas, Wassgren and Sadeghi [18] found both analytically and experimentally that, in a small axial load condition, cage center oscillates in a small amplitude, but, in a large axial load condition, this motion becomes unbalanced and unpredictable.

5.3 High accelerations and skidding

In bearings operating at high speeds, the force created by the rolling element moving mass causes significant additional internal loads at the cage-rolling element contacts. Especially in cylindrical roller bearings the acceleration of the rolling elements requires a large amount of energy. A further issue directly associated to the mass inertia of rollers and cage is the sliding friction that frequently occurs in rolling bearings that are insufficiently loaded or accelerated too quickly, which, in extreme cases, may destroy the bearing precision-finished raceway surfaces.

Skidding is a very gross sliding condition occurring generally in oil-film lubricated ball and roller bearings operating under relatively light loads at very high speeds or rapid accelerations and decelerations. When skidding occurs, cage speed will be less than predicted by simple kinematics equations. In the bearing industry it is quite common to measure the cage speed by means of the cage slip defined as:

$$cage\_slip = 1 - \frac{\omega_{cage}}{\omega_{cage\_nominal}} \tag{7}$$

where ω_{cage} is the mean cage speed and $\omega_{cage\_nominal}$ is the nominal cage speed given by the simple kinematics Eq. (4). A cage slip of 0.3 (or 30%) therefore corresponds to a cage speed equal to 70% of its nominal value.

Numerical results obtained by Houpert with CAGEDYN simulation software, as well as experimental measurements carried out by Lang and Witte by using a high-speed camera [16], [17], showed that slip occurs at light load and high speed, mainly at the roller-inner race contact, leading to a smaller average roller orbital speed and hence smaller cage speed. Comparative results for inch-size bearing series 74000 are shown in Fig. 9.

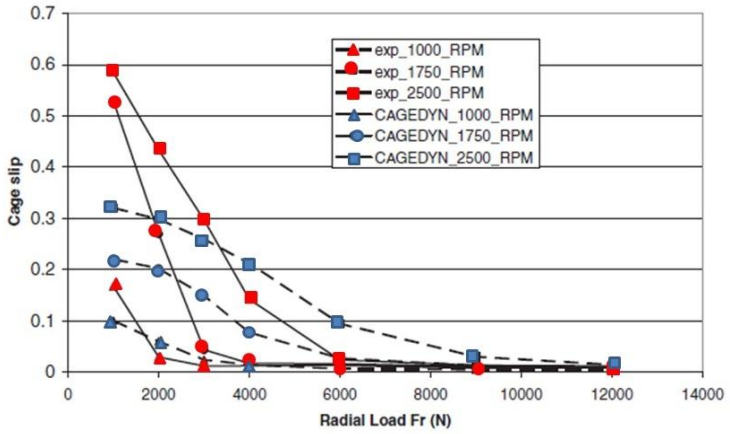

Fig. 9 – Calculated and measured cage slip for inch size tapered roller bearing 74000

If, during operation, the load on cylindrical roller bearings becomes too small, slippages occurring in the roller-raceway contacts may result in smearing.

Due to the traction force in the load zone, the roller speed tends to accelerate in the load zone to reach its nominal value, leading to one or multiple roller-cage bridge impacts during the excursion of the roller through the load zone.

Cages in bearings subject to severe accelerations and slowdowns in conjunction with fluctuations in speed are affected by forces of inertia, that eventually give rise to considerable pressure between the contacting surfaces, with consequent heavy wear and smearing.

5.4 Gyroscopic motion

In ball bearings with non-zero contact angles between balls and raceways, during operation at any shaft or outer ring speed, a gyroscopic moment occurs on each loaded ball, tending to cause a sliding motion [1], [3].

In most applications, because of relatively slow input speeds or heavy loading, such gyroscopic moments and hence motions can be neglected. In high-speed applications with oil-film lubrication between balls and raceways such motions occur.

6 CAGE DYNAMICS AND IMPACT FORCES

The problem of cage dynamics and impact forces can be reduced to the case of a roller of mass m_1 and initial speed v_{1i} hitting a cage bridge of mass m_2 (Fig. 10 and Fig. 11).

A realistic cage dynamic model has to take into considerations the following elements:

- The appropriate cage stiffness.
- The calculation of the roller-race traction forces.
- The use of hydrodynamic roller-race or roller-cage bridge load.

6.1 Stiffness model

The use of an appropriate roller-cage contact stiffness is essential when deriving the cage bridge impact load and corresponding cage stresses. If a rather simple model, based on the traditional Hertzian contact stiffness only, is used [20], then too large impact forces result in a very short impact time, incompatible with the low vibration frequency of the bridge bending mode.

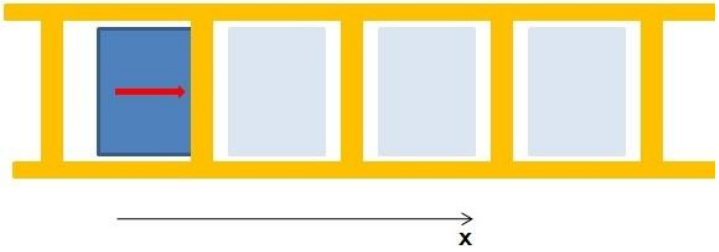

Fig. 10 – Roller-cage impact

An elastic system with two degrees of freedom that considers both roller-cage Hertzian stiffness K_H and cage structural stiffness K_S (Fig. 11) proved to be a better representation for the roller-cage contact [16].

Elastic deformation of metals is accompanied by a very small hysteresis that allows to neglect the structural damping. The gravity effects are also negligible.

The contact stiffness K_H is derived from the Hertzian contact theory [21], whereas the structural bridge stiffness K_S can be obtained analytically or numerically using the finite element analysis if the bridge shape is complex.

The stiffnesses K_H and K_S are used further for assessment of the Hertzian load Q_1 and the bridge load Q_2 responsible for its bending. The bridge load Q_2 will be the load used to calculate the reaction forces at the bridge.

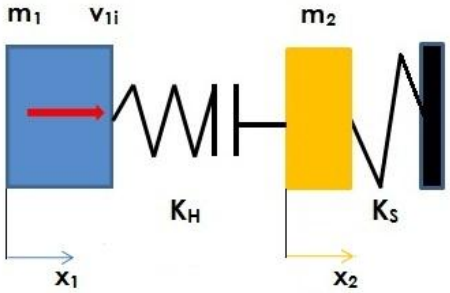

Fig. 11 – Model of the roller-cage impact dynamic simulation

Note that the bridge mass and stiffness are reduced to the point of contact so that the bridge mass m_2 is, for example, not equal to the true bridge mass. The use of super-element techniques (classical stiffness and mass condensation technique) is needed to define the reduced stiffness K_S and mass m_2 .

The dynamic equilibrium condition written for each of the two masses provides the following set of two differential equations:

$$K_H.(x_1 - x_2)^n + m_1 \frac{\mathrm{d}^2 x_1}{\mathrm{dt}^2} = 0 \tag{8}$$

$$-K_H.(x_1 - x_2)^n + K_s.x_2 + m_2.\frac{\mathrm{d}^2 x_2}{\mathrm{dt}^2} = 0 \tag{9}$$

The solution x_1 and x_2 are obtained by integrating versus time these two differential equations with initial condition $V_1 = V_{1i}$, at time $t = 0$.

The typical result presented in Fig. 12 highlights that, instead of a single impact, multiple short contacts are possible at the roller-bridge Hertzian contact, while the bridge load is deployed during a longer time, of the order of 3.5E-4 s [16].

6.2 Distribution of the normal forces

In most cases the load distribution in a rolling element bearing may be approximated by the load distribution in a statically loaded bearing. Subsequently, in order to obtain the dynamic load distribution, the centrifugal force acting

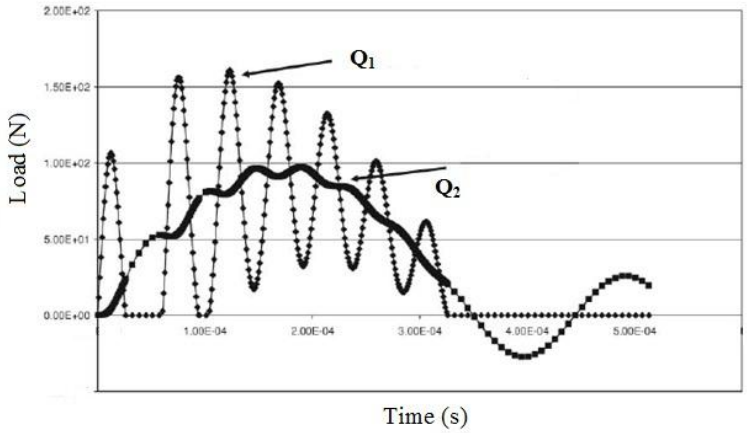

Fig. 12 – Hertzian load Q_1 and bridge load Q_2

on the rollers can be added to the static load distribution on the outer raceway. A schematic representation of the different contributions to the load distribution, for a bearing under pure radial load F_r, is shown in Fig. 13. The angle Ψ denotes the angular position along the circumference of the bearing. Depending on the angle Ψ, it is possible to distinguish three regions, where different contributions act:

- Static load distribution on the inner raceway $\Psi \in [-\Psi l, \Psi l]$.
- Static load distribution and centrifugal force on the outer raceway $\Psi \in [-\Psi l, \Psi l]$.
- Centrifugal force on the outer raceway $\Psi \in [-\Psi l, 2\pi - \Psi l]$.

For a rigidly supported bearing subjected to a radial load F_r, the static load distribution is given in classic rolling bearing handbooks [1], [3]:

$$Q_i(\psi) = Q_{max}\left(1 - \frac{1}{2\varepsilon}\left(1 - \cos(\psi)\right)\right)^n \tag{10}$$

where Q_{max} is the maximum static load, and ε is the load distribution factor determining the size of the load zones I and II, that is 2Ψ (Fig. 13). The power n is 1.5 for circular and elliptical contacts and 1.11 for line contacts.

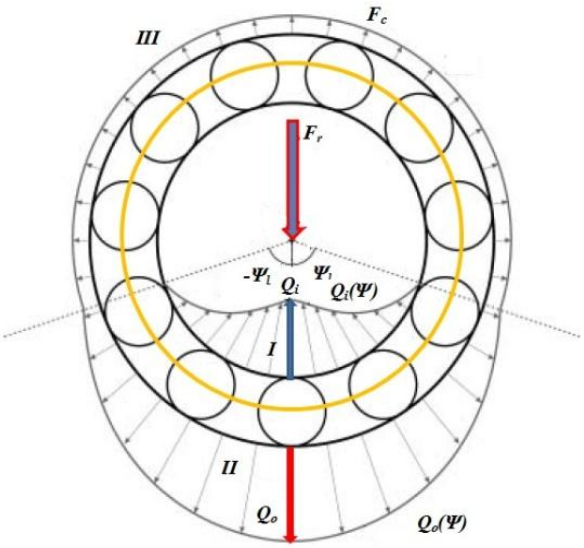

Fig. 13 – Load distribution on the inner raceway $Q_i(\Psi)$ and the outer raceway $Q_o(\Psi)$

The undimensional ε is a function of the radial load F_r, the number of rolling elements Z, the load deflection factor (contact stiffness) K_n , and the diametral clearance P_d. Iterative methodologies are presented in [1], [3] but also in ISO 16281:2008 [7].

The load distribution on the outer raceway is obtained by adding the centrifugal force F_c to the static load distribution:

$$F_o(\psi) = F_i(\psi) + F_c \tag{11}$$

The centrifugal force that acts on the outer contact of a roller is proportional to the mass of the rolling element m_w times its acceleration:

$$F_c = m_w \cdot \omega_c^2 \cdot \frac{D_{pw}}{2} \tag{12}$$

Since there is a clearance between the roller and the raceways, the roller inner raceway load Q_i is therefore nil in the unloaded zone.

6.3 Roller-race traction force

The tangential forces acting in the orbital direction x, are: F^R, F^P, and F^S as shown in Fig. 14. Their resultant plays a major role in development of the roller orbital and rotational accelerations, and consequently alters the roller speed from the value provided by Eq. (5).

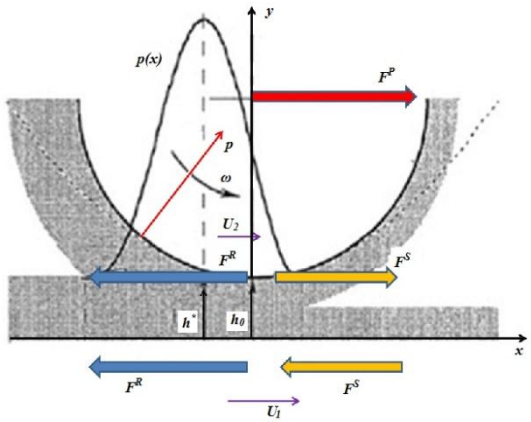

Fig. 14 – Description of the hydrodynamic rolling and pressure force and sliding force

The resistance force F^R is the main braking force developed in the inlet of the lubricated contact. Likewise for the film thickness, the resistance force F^R can be calculated as a function of the three dimensionless parameters *U, G,* and *W* and are proportional to the contact length *L*. In the *EHD* line contact regime, Houpert [16] suggests the following relationship:

$$F^{\mathrm{R}}_{\mathrm{EHD}} = 0.04\, E_{\mathrm{eq}} \cdot R_{\mathrm{x}} \cdot U^{0.44} \cdot W^{0.37} \cdot L \tag{13}$$

The force F^P is due to the nonsymmetrical pressure distribution and the pressure component in the x direction. Since the pressure points towards the roller center, this force does not contribute to the moment applied at the roller center. It is possible to express F^P as a function of F^R and the contacting surface radii.

The derivation of the sliding force F^S is quite difficult requiring use of nonlinear models as those used in the EHD regime [22].

6.4 Experimental validation of the roller-cage impact forces

Roller-cage bridge impact forces have been measured and described by Lang and Witte [16]. The data presented in Fig. 15 reveals the quite good correlation between the measured and computed data and validates the simulation model for the cage dynamic behavior.

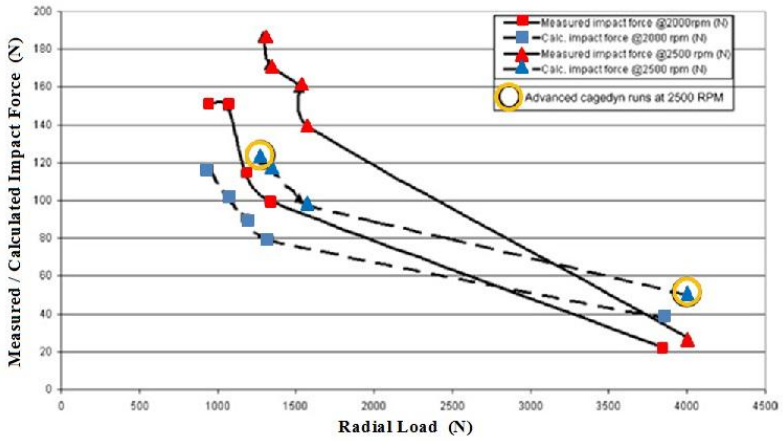

Fig. 15 – Measured and calculated roller-cage impact forces

Both the experimental measurements and CAGEDYN simulation pointed out that the roller-cage impact forces increase when the radial load decreases. As a result, low bearing loads are to be avoided because they contribute to cage slip and cage failure.

7 MEASURES TO AVOID ADHESIVE WEAR AND SMEARING AT ROLLER-CAGE IMPACT

The impact between cage and rolling element is normally achieved with significant but inevitable sliding velocities, Eq. (5). Consequently, a certain form of cage wear may occur and evolve to destructive smearing if, in conditions of poor lubrication, high values of contact pressure between collision surfaces arise. The skewing motion of the rolling element, as well as the high collision forces due to the inertia effects, generate the contact pressures able to produce cage smearing.

To avoid adhesive bonding between material portions of the contacting surfaces some measures, it is highly advisable to:

- Select a cage material able to ensure, against hardened steel and in boundary lubrication regime, reduced values for the friction coefficient as well as a very high resistance to welding. In this regard, brass proved to be the best choice.
- Design solutions to improve lubrication in the critical contact areas between cage and rolling element.
- Treat surfaces to further reduce friction and wear. To improve sliding and wear resistance properties some machined steel cages need surface treatment.

In contact with hardened steel roller the brass cage has a much higher resistance to adhesive bonding compared to the pressed steel cage. For this reason, brass cage bearings can attain the calculated rating life according to ISO 281:2007, even in conditions of boundary lubrication. This type of cage also gives early warning of potential failure, so that service time can be scheduled cost-effectively.

CONCLUSIONS

The equations mentioned in the international standards ISO 281:2007 and ISO 16281:2008 for computing bearing dynamic load ratings are based on the assumption that origin of any failure is the subsurface contact fatigue of raceways. To consider the surface originated failures, the rating life equation contains the life modification factor a_{ISO} that, besides bearing type, fatigue load and bearing load, quantifies the quality of lubrication, contamination level and contaminant particles. Both the dynamic load rating and rating life equations contain no difference regarding cage design and material (brass or steel). Consequently the cage design has evolved to achieve higher and higher bearing load rating capacities, by incorporating more rollers, and lower costs, by replacing brass with cheaper low carbon steel, probably also for reasons connected to the economies of scale pursued by the biggest bearing manufacturers.

Numerical simulations and experimental studies showed that in the loaded zone, due to the traction forces, the roller speed tends to accelerate to reach its nominal value, which leads to single or multiple roller-cage bridge impacts. In the case of roller bearings, the existence of skewing motion alters the line contact to the harmful edge type contact and subsequently the interaction force develops a much higher contact pressure.

When a rolling bearing equipped with a steel cage works in condition of poor lubrication, hard contaminants might appear as a result of the adhesive wear at the cage-rolling element contact, which generates indentations on raceways and rolling elements that may lead to a much shorter life than that calculated using ISO 281:2007. On the contrary, brass cages have a much higher resistance to adhesive bonding compared to steel cages. Therefore, the bearings equipped with a machined brass cage are able to provide the calculated rating life according to ISO 281:2007 even in harsh conditions and in case of deficient lubrication.

REFERENCES

[1] T. A. Harris and M. N. Kotzalas, *Rolling Bearings Analysis – Advanced Concepts of Bearing Technology*, Taylor & Francis Group, 2007.
[2] D. Nelias, "Contribution a l'etude des roulements", Dossier d'habilitation a diriger des recherché, Laboratoire de Mecanique des Contacts, INSA de Lyon, 5514, December 1999.
[3] M. Gafitanu, D. Nastase, S. Cretu, and D. Olaru, *Rulmenti – Proiectare si tehnologie*, vol. 1, Editura Tehnica, Bucuresti, 1985.
[4] E. Ioannides, G. Bergling, and A. Gabelli, "An analytical formulation for the life of rolling bearings", *Acta Polytechnica Scandinavica*, vol. 137, pp. 1–80, 1999.
[5] G. Morales-Espejel, A. Gabelli, and E. Ioannides, "Micro-geometry lubrication and life ratings of rolling bearings", *J. Mech. Eng. Science,* vol. 224(12), pp. 2610–2626, 2010.

[6] ISO 281:2007, *Rolling bearings – Dynamic load ratings and rating life*.
[7] ISO/TS 16281:2008, *Rolling bearings – Methods for calculating the modified reference rating life for universally loaded bearings.*
[8] ISO 15243:2004, *Rolling bearings – Damage and failures – Terms, characteristics and causes*.
[9] T. A. Harris, M. N. Kotzalas and W. K. Yu, "On the causes and effects of roller skewing in cylindrical roller bearings", *ASME Tribology Transactions*, vol. 41, 4, pp. 572–578, 1998.
[10] A. P. Noronha, "Rechnerische Simulation des Betriebsverhaltens von Pendelrollenlagern", *Walzlagertechnik Industrietechnik*, vol. 501, pp. 11–18, 1990.
[11] Y. Yang, S. Danyluk, and M. Hoeprich, "Rolling element skew in tapered roller bearings", *STLE Presentations*, Nashville, Tennessee, Preprint 00-AM-16, 2000.
[12] S. Cretu, I. Bercea, and N. Mitu, "A dynamic analysis of tapered roller bearings under fully flooded conditions. Part 1: Theoretical formulation", *WEAR*, 188, pp. 1–10, 1995.
[13] S. Cretu, I. Bercea, and N. Mitu, "A dynamic analysis of tapered roller bearing under fully flooded conditions. Part 2: Results", *WEAR*, 188, pp. 11–18, 1995.
[14] I. Bercea, S. Cretu, and D. Olaru, "Simulating roller-cage pocket friction in a tapered roller bearing", *European Jour. of Mech. Eng.*, 43, pp. 189-194, 1998.
[15] T. Sakaguchi, K. Harada, "Dynamic analysis of cage behavior in a tapered roller bearing," *ASME Tribology Transactions*, vol. 128, pp. 604–611, 2006.
[16] L. Houpert, "CAGEDYN: a contribution to roller bearing dynamic calculations. Part I: Basic tribology concepts", *ASME Tribology Transactions*, vol. 53, pp. 1–9, 2010.
[17] L. Houpert, "CAGEDYN: A contribution to roller bearing dynamic calculations. Part III: Experimental validation", *ASME Tribology Transactions*, vol. 53, pp. 848–859, 2010.
[18] N. Ghaisas, C. R. Wassgren, and F. Sadeghi, "Cage instabilities in cylindrical roller bearings", *ASME Journal of Tribology*, vol. 126, pp. 681–699, 2004.
[19] E. Ioannides, "EHL in rolling element bearings, recent advances and the wider implications", *Proceedings of the 23rd Leeds-Lyon Symposium of Tribology*, University of Leeds, UK, 10–13 Sept. 1996, in D. Downson et al. (editors) *Elastohydrodynamics* 96, Elsevier Science B.V., pp. 3–12, 1997.
[20] K. Gupta, *Advanced dynamics of rolling elements*, Springer-Verlag, Berlin, 1984.
[21] S. Cretu, *Contactul Concentrat Elastic-Plastic*, Polytehnium, Iasi, 2009.
[22] D. Nelias, E. Legrand, P. Vergne, and J. Mondier, "Traction behavior of some lubricants used for rolling bearings in spacecraft applications: experiments and thermal model based on primary laboratory data", *ASME Journal of Tribology*, vol. 72, pp. 72–81, 2002.